



# Margins of Planning Target Volume and Set-up Errors based on Megavoltage Cone-Beam CT Image Guided Radiotherapy with Helical Tomotherapy: Importance of Automatic Registration Plus Manual Registration

Danial Seifi Makrani (PhD Candidate)<sup>1,2</sup>, Nooshin Banaee (PhD)<sup>3</sup>, Ghazale Geraily (PhD)<sup>1,2</sup>, Hassan Ali Nedaie (PhD)<sup>1,2\*</sup>, Alireza Khorrami Moghaddam (PhD)<sup>4</sup>, Hussam Hameed Jassim (PhD)<sup>1,2,5</sup>

## ABSTRACT

**Background:** Helical Tomotherapy (HT) enables daily verification of patient positioning using Megavoltage Computed Tomography (MVCT) during each treatment session.

**Objective:** The present study aimed to investigate the effects of Automatic Registration (AR) compared to a combination of Automatic and Manual Registration (AR+MR) on setup errors. Additionally, the study aimed to determine the corresponding Margins of the Planning Target Volume (MPTV).

**Material and Methods:** In this experimental study, a total of 1513 daily MVCT scans were analyzed from September 2020 to January 2024, which were obtained from 71 patients diagnosed with Head and Neck (HN), cervical, and gastrointestinal cancer. The scans were registered with the planning CT to determine the setup errors of the patients. The analysis compares the setup errors between the AR and the AR+MR techniques in translational (X, Y, and Z axes) and rotational directions ( $R_x$ ,  $R_y$ , and  $R_z$ ). Additionally, the study calculated the MPTV.

**Results:** In the AR and AR+MR techniques, the translational setup errors were significantly different in the Z-axis for HN patients. For cervical cancer patients, AR and AR+MR exhibited significantly different translational errors across all axes. Furthermore, they also had notable differences in the Y and Z-axis translational errors for Gastro-Intestinal (GI) patients. Regarding the rotational setup errors, a substantial difference was observed in the Z-axis translational error for cervical cancer patients, and in the Y and Z-axes for GI patients.

**Conclusion:** Human assessment after automatic registration helps ensure that the registration is clinically appropriate, especially in circumstances involving deformable patient anatomy.

## Keywords

Radiotherapy; Image-Guided; Cone-Beam Computed Tomography; Radiotherapy Setup Errors

<sup>1</sup>Department of Medical Physics and Biomedical Engineering, School of Medicine, Tehran University of Medical Sciences, Tehran, Iran

<sup>2</sup>Radiation Oncology Research Center, Cancer Institute, Tehran University of Medical Sciences, Tehran, Iran

<sup>3</sup>Medical Radiation Research Center, Central Tehran Branch, Islamic Azad University, Tehran, Iran

<sup>4</sup>Department of Radiology, Faculty of Allied Medicine, Mazandaran University of Medical Sciences, Sari, Iran

<sup>5</sup>Department of Radiotherapy Physics, General Al-Najaf Al-Ashraf Hospital, Najaf, Iraq

\*Corresponding author: Hassan Ali Nedaie  
Department of Medical Physics and Biomedical Engineering, School of Medicine, Tehran University of Medical Sciences, Tehran, Iran  
E-mail: nedaieha@sina.tums.ac.ir

Received: 3 March 2024

Accepted: 27 April 2024

## Introduction

Modern radiotherapy technology can precisely conform higher radiation doses to the target volume while effectively sparing normal tissues [1-4]. Immobilization devices, such as the thermoplastic mask and vacuum cushion, have long been employed to obtain great positional repeatability [5, 6]. However, in clinical positioning practice, mismatches between the patient surface and the immobilization device result in visible interfraction setup errors [7, 8]. In radiotherapy, image guidance is routinely utilized to identify big setup problems and fine-tune patient location [9, 10]. Image-guided Radiation Therapy (IGRT) uses onboard imaging technologies, including Cone-beam Computed Tomography (CBCT) and Electronic Portal Imaging Device (EPID) to increase radiotherapy setup accuracy [11]. Despite image guidance, everyday alterations in patient setup are unavoidable [12]. The IGRT system, including daily monitoring of patient position on the treatment machine using X-ray images, can lead to minimizing geometrical errors caused by intra and interfraction motion [13]. The reduction of interfraction systematic and random errors results in the narrowing of the margins between the Clinical Target Volume (CTV) and the Planned Target Volume (PTV) [14, 15]. To account for systematic and random mistakes in daily setup and guarantee an appropriate dose to target tissue, the PTV adds a margin into the CTV known as the Margin of Planned Target Volume (MPTV) [16-19]. Currently, MPTV is generally 10 mm in the absence of remedial interventions [20]. Consequently, it is crucial to assess intrafraction motion individually for each specific tumor location and patient immobilization method. In this study, MVCT images, obtained from the Helical Tomotherapy (HT) system (Accuray, Sunnyvale, CA, USA), were utilized to compare the variations in position errors between automatic registration (AR) and automatic plus manual registration (AR+MR). The study

aimed to provide a benchmark for determining the MPTV in HT treatment for patients diagnosed with HN, cervical, and Gastrointestinal (GI) cancers.

## Material and Methods

### Patient characteristics

In this experimental study, a total of 71 patients participated, who underwent treatment with HT at the Mazandaran Radiotherapy Center between September 2020 and January 2024 (ranging in age from 30 to 82 years old). The patients were categorized based on their cancer types, specifically HN, cervical, and GI cancers. MVCT scans of these patients were analyzed as part of the study. All patients underwent HT with 6 MV photon beams and daily fan beam MVCT imaging guiding. The MVCT image slice width includes three options; coarse (6 mm), normal (4 mm), and fine (2 mm) mode. The images were obtained in normal mode at the center. The duration of imaging may vary based on the thickness of the slice and the length of the scanned area. Furthermore, HT uses a binary Multi-leaf Collimator (MLC) to produce helical highly modulated IMRT plans. The MLC has 64 interleaved leaves that measure 6.25 mm in width at the isocenter. It is important to highlight that patients, who had dental implants (which could cause metal artifacts) and MVCT images with any kind of artifacts, were excluded from the study. Additionally, only patients with a minimum of 20 sets of daily MVCT images were included in the dataset.

#### a) Head and Neck Patients

Twenty-five HN patients, comprising glioblastoma (14), neuroblastoma (2), and meningioma (9), received Intensity Modulated Radiotherapy (IMRT) with HT. The patient was positioned supine, supported by a headrest and a thermoplastic immobilization shell (Orfit, Jericho, NY, USA).

#### b) Cervical cancer patients

All twenty-four cervical patients were

pathologically confirmed, including 18 squamous cell carcinoma, 4 adenocarcinoma, and two cervical intraepithelial neoplasia grade III cases. During the treatment, the patients were set in a supine position on a carbon fiber body frame and secured with a thermoplastic body membrane. The placement was simulated using a CT simulator to ensure consistency and accuracy throughout the treatment process.

### c) Gastrointestinal sufferers

This research included twenty-two consecutive GI cancer patients, including 10 cases of esophageal cancer, 2 Pancreatic cancer, and 7 Gastric cancers. All patients had non-metastatic cancer at stage T3 or T4, with an unresectable or borderline unresectable illness. Every patient has normal functioning in both kidneys. The patients were positioned supine, with both hands on the elbows, and the thermoplastic body fixator was used to secure the patient's position.

### Image Acquisition, Planning, and Verification

The CT images were obtained on a computed tomography machine (Siemens, Germany) using a matrix of  $512 \times 512$  with a voxel size of  $0.976 \times 0.976 \times 3 \text{ mm}^3$  that was transferred via DICOM local area network to the planning system process to produce the treatment plan. The target region was defined using the ICRU-83 reporting standard. The study involved defining the Gross Tumor Volume (GTV), Clinical Target Volume (CTV), Planning Target Volume (PTV), and Organs at Risk (OARs). The medical physicist was responsible for designing the treatment plan, which was then evaluated by the supervising physician and physicist collaboratively. To ensure accurate patient alignment during each treatment fraction, daily MVCT images were captured using the HT unit. The images were obtained with a  $512 \times 512$  matrix and voxel dimensions of  $0.763 \times 0.763 \times 4 \text{ mm}^3$ . These images served as a reference for aligning the patient and verifying the correct positioning before each

treatment session. Typically, the MVCT scan range includes the whole GTV, CTV, and OARs. MVCT images were rebuilt and compared to the positioned planning CT image. The HT treatment planning system employs over appropriate landmarks for each disease site, and the positions of PTV (both bone landmarks and soft tissue) in AR mode involve assessing the supra-orbital ridge, which stays undamaged within the immobilization mask, as well as the chin and other stable anatomical structures. The bone features around the PTV were regarded as landmarks for cervical and GI patients. After AR was finished, the position error values were calculated for the three linear directions and angular rotations of the left and right (X), head and feet (Y), and abdominal back (Z) axis directions, as well as rotating coronal position ( $R_x$ ), sagittal position ( $R_y$ ), and transverse position ( $R_z$ ). The unit of translational heading was millimeter (mm), though the unit of turning heading was degree ( $^\circ$ ). The overlap between the MVCT image and the anticipated CT image was then calculated, and manual registration was used as needed until the registration result matched the criteria. The record applies the most recent automated positioning + manual allocation error (AR+MR) to the radiation treatment bed. A third-party verification system called the Delta4 Phantom (ScandiDos, Sweden) is employed, before commencing the treatment.

### MPTV determination

According to the International Commission on Radiation Units and Measurements (ICRU) Report No. 62 [21], the left side of the x-axis is positive; the upper side of the y-axis is positive; the front side of the z-axis is positive and the rear side is negative. Finally, the angle of rotation is positive when the upper end is tilted toward the foot and the lower end is tilted toward the foot.

$\Sigma$  and  $\delta$  indicate systematic and random errors, respectively. Van Herk's [22] research found that the formula for CTV to

PTV expansion in X, Y, and Z directions was  $MPTV=2.5\Sigma+0.7\delta$ , where  $\delta$  is the root mean square of the individual random error.

### Statistical Processing

The data was reported as  $x\pm s$ . SPSS software (version 20.0) was used to compute  $\Sigma$  and  $\delta$  in each direction. A paired t-test was utilized to compare the AR positioning error value with the automatic-assisted manual registration position error.  $P$ -value $<0.05$  indicates statistical significance.

## Results

### General Data

A total of 1513 eligible CBCT scan results were collected, with each patient receiving 20-25 treatment fractions. The scans were obtained from 530 HN-cancer, 502 cervical-cancer, and 481 GI-cancer patients. For detailed data, please refer to Table 1.

### Comparison of Translational Setup Errors for AR and AR+MR Values

The AR and AR+MR values in translational setup errors for HN, cervical, and GI cancer cases are shown in Table 2. According to Table 2, the X, Y, and Z axis translational setup errors for HN patients with AR were -1.1 mm, -0.2 mm, and 1.5 mm, respectively. HN patients with AR+MR had X, Y, and Z axis translational setup errors of -0.7 mm, 0.3 mm, and

0.2 mm, respectively. There was a significant difference between AR and AR+MR translational setup error in the Z-axis ( $P$ -value $<0.05$ ). However, there was no statistical significance between AR and AR+MR position error values on the x and y axes ( $P$ -value $>0.05$ ). Results of Table 2 show that cervical patients with AR had X, Y, and Z axis translational setup errors of -2.1 mm, 3.5 mm, and 2.2 mm, respectively. The cervical cancer patient with AR+MR had X, Y, and Z axis translational setup errors of -0.1 mm, 1.4 mm, and 0.5 mm, respectively. AR and AR+MR showed significantly different translational errors across all axes ( $P$ -value $<0.05$ ). Finally, for GI cases, results show that GI patients with AR had X, Y, and Z axis translational setup errors of -1.1 mm, -1.4 mm, and 1.7 mm, respectively. The GI patient with AR+MR had X, Y, and Z axis translational setup errors of -0.7 mm, 0.5 mm, and 0.1 mm, respectively. There was a substantial difference in Y and Z-axis translational errors between AR and AR+MR ( $P$ -value $<0.05$ ).

### Comparison of Rotational Setup Errors for AR and AR+MR values

The AR and AR+MR values in rotational setup errors for HN, cervical, and GI cancer cases are shown in Table 3. According to Table 3, the rotational setup blunders of HN cases with AR were 0.76, -1.04, and 1.07 degrees, respectively. The  $R_x$ ,  $R_y$ , and  $R_z$  rotational setup errors in AR+MR were 0.52,

**Table 1:** The collected data of the patients.

	Head & Neck patients	Cervical cancer patients	Gastrointestinal patients
Number of Patient	25	24	22
Median Age	52.5	48.3	53.2
Tumor type	Glioblastoma (14) Neuroblastoma (2) Meningioma (9)	cases of squamous cell carcinoma (18), adenocarcinoma (4), cervical intraepithelial neoplasia (2)	Esophageal cancer (10) Pancreatic cancer (5) Gastric cancer (7)
Number of CBCT	530	502	481

CBCT: Cone-beam Computed Tomography

**Table 2:** Comparison of translational errors between the two groups for all patients

Translational errors					
Case	Group	Number of CBCT	X (range)	Y (range)	Z (range)
HN Patients	AR	530	-1.1 (-2.5,3.5)	-0.2 (-1.7,1.3)	1.5 (-1.5,3.8)
	AR+MR	530	-0.7 (-1.4,2.6)	0.3 (-0.1,1.1)	0.2 (-0.8,1.4)
	T		-2.2	1.5	4.2
	<i>P</i> -value		0.65	0.225	0.001
Cervical patients	AR	502	-2.1 (-4.7,0.8)	3.5 (-1.1,5.0)	2.2 (-1.4,4.6)
	AR+MR	502	-0.1 (-1.1,0.6)	1.4 (-0.2,2.3)	0.5 (-0.3,1.8)
	T		-1.5	2.8	3.2
	<i>P</i> -value		0.01	0.006	0.005
GI patients	AR	481	-1.1 (-2.3,1.1)	-1.4 (-3.1,3.5)	1.7 (-0.8,4.2)
	AR+MR	481	-0.7 (-1.2,1.3)	0.5 (-0.7,1.1)	0.1 (-0.6,1.3)
	T		-2.2	3.2	4.8
	<i>P</i> -value		0.86	0.02	0.001

CBCT: Cone-beam Computed Tomography, HN: Head&Neck, AR: Automatic Registration, MR: Manual Registration, GI: Gastrointestinal

**Table 3:** Comparison of rotational errors between the two groups for all patients

Rotational errors					
Case	Group	Number of CBCT	X (range)	Y (range)	Z (range)
HN Patients	AR	530	0.76 (0.35,1.72)	-1.04 (-1.8,1.2)	1.07 (0.5,1.8)
	AR+MR	530	0.52 (-0.19,1.2)	-0.51 (-1.1,0.2)	0.81 (0.3,1.42)
	T		1.2	2.6	3.7
	<i>P</i> -value		0.36	0.44	0.54
Cervical patients	AR	502	1.23 (0.5,2.79)	1.08 (-0.5,1.9)	1.43 (0.8,1.95)
	AR+MR	502	0.71 (0.4,1.6)	0.84 (-0.2,1.08)	0.51 (0.1,0.88)
	T		1.19	1.18	3.2
	<i>P</i> -value		0.24	0.25	0.004
GI patients	AR	481	0.95 (0.5,2.15)	1.04 (-0.5,1.5)	1.25 (0.2,1.65)
	AR+MR	481	0.55 (0.1,1.4)	0.62 (-0.3,1.1)	0.36 (0.1,0.65)
	T		0.83	2.97	2
	<i>P</i> -value		0.40	0.03	0.02

CBCT: Cone-beam Computed Tomography, HN: Head & Neck, AR: Automatic Registration, MR: Manual Registration, GI: Gastrointestinal

-0.51, and 0.81 degrees, respectively. The two registration approaches showed no significant variations in rotational error ( $P$ -value>0.05). Cervical cancer patients with AR had  $R_x$ ,  $R_y$ , and  $R_z$  rotational setup errors of 1.23, 1.08, and 1.43 degrees. The rotational setup errors in AR+MR were 0.71, 0.84, and 0.51 degrees, respectively. Both groups showed a significant dissimilarity in Z-axis translation error ( $P$ -value<0.05). The rotational setup inaccuracies of GI cases with AR were 0.95, 1.04, and 1.25 degrees, respectively.  $R_x$ ,  $R_y$ , and  $R_z$  rotational setup errors in AR+MR were 0.55, 0.62, and 0.36 degrees, respectively. The Y and Z-axes translational errors differed significantly between the two clusters ( $P$ -value<0.05).

### Comparison of MPTV Values Systematic and random error computation

For each individual case, all movements and displacements were recorded in the X, Y, and Z axes and the average displacement was determined.

The mean (M) of the averages and Standard Deviation (SD) for each axis were then calculated. The systematic error ( $\Sigma$ ) was estimated by calculating the standard deviation of averages (m) for each axis. The random error ( $\sigma$ ) is calculated by taking the square root of the average of the SD<sup>2</sup> per axis. Table 4 shows the expansion boundaries beyond the target region for all patients with AR and AR+MR. According to this, results show that the

**Table 4:** Margins of Planning Target Volume (MPTV) of Clinical Target Volume (CTV) to Planning Target Volume (PTV expansion boundary for all Patients in different registration methods

Case	Group	Axis	$\Sigma$	$\Sigma$	MPTV=2.5 $\Sigma$ +0.7 $\sigma$
HN Patients	AR	X	0.92	1.14	3.098
		Y	1.26	1.31	4.067
		Z	2.26	2.44	7.358
	AR+MR	X	0.87	0.91	2.812
		Y	1	1.29	3.403
		Z	1.43	1.04	4.303
Cervical patients	AR	X	1.26	1.22	4.004
		Y	2.51	1.64	7.423
		Z	2.7	2.1	8.22
	AR+MR	X	1.08	0.93	3.351
		Y	1.4	0.97	4.179
		Z	1.67	1.34	5.113
GI patients	AR	X	1.41	0.94	4.183
		Y	2.94	3.12	9.534
		Z	1.95	3.55	7.36
	AR+MR	X	1.29	0.8	3.785
		Y	1.66	1.32	5.074
		Z	1.65	1.06	4.867

MPTV: Margins of Planning Target Volume, CTV: Clinical Target Volume, PTV: Planning Target Volume, HN: Head & Neck, AR: Automatic Registration, MR: Manual Registration, GI: Gastrointestinal

expansion boundaries beyond the target region for HN patients with AR and AR+MR were X (3.098, 2.812) mm, Y (4.067, 3.403) mm, and Z (7.358, 4.303) mm, respectively. The expansion boundary beyond the target region of cervical cancer patients with AR and AR+MR were X (4.004, 3.351) mm, Y (7.423, 4.179) mm, and Z (8.22, 5.113) mm; finally, the expansion boundaries beyond the target region of the GI patients with AR and AR+MR were X (4.183, 3.785) mm, Y (9.534, 5.074) mm, and Z (7.36, 4.867) mm, respectively.

## Discussion

More modern approaches, such as IMRT or Adaptive Radiation Therapy (ART), may provide highly conformal dose distributions with better target volume coverage and normal tissue sparing than traditional procedures [23-25]. These approaches can enhance treatment results while dramatically lowering the dose of OARs [26]. Nonetheless, inconsistencies in inter-fraction placement may result in dose mistakes; the steepness of the dose-effect curves might restrict IGRT effectiveness, influencing patient outcomes for both local tumor reduction and normal tissue consequences [27, 28].

For HN patients, the superior and inferior shifts play a significant role in tumor underdose [29]. A 3-millimeter setup mistake in the posterior and lateral orientations considerably affects the dose of the spinal cord [30, 31]. Likewise, setup mistake in the lateral and anterior orientations influences the dose to both parotids [32]. Similarly, in the treatment of GI malignancies, the radiation dose administered to the lung and heart should be monitored, since even modest doses of radiation to the lung may cause significant harm [33]. Research indicated that dose discrepancies in the thoracic region, especially in the supine position might be linked to the patient setup [34].

Image registration may help to ensure that the target region and OAR are as close to the intended location as feasible during

fractionated treatments [35]. The HT image guiding feature, enables real-time image registration, instantly determines the error value of the treatment, and applies it to the treatment plan, making the registration easy and fast. Manual registration necessitates a visual evaluation of the overlap between the anatomical structure and the area of interest, which takes time, puts a strain on technicians, and necessitates clinical verification [36].

In order to calculate the appropriate PTV margin, the inter-fractional setup errors of patients should be analyzed when applying a new treatment technique, such as a new generation of tomotherapy machine and new-fangled immobilization device or extending the indication of the technique to malignancies at other sites. [37]. The current study aimed to determine setup errors in all three dimensions as well as final CTV-PTV margins. Daily setup was recorded in all three dimensions (X, Y, and Z), and CBCT images were matched using bone landmarks and soft tissues. That would be a reference for clinical practice and future development of artificial intelligence neural networks for patients undergoing tomotherapy.

### Head and Neck cases

The implementation of AR+MR registration led to a reduction in both systematic and random uncertainties. However, when specifically analyzing the HN patients, the results indicated no significant difference between AR and AR+MR registration in terms of translational and rotational setup errors, except for a significant difference observed in the Z-axis. This discrepancy could potentially be attributed to the utilization of a headrest and a thermoplastic immobilization shell for body fixation during radiotherapy. These immobilization devices may have contributed to the observed variation in the Z-axis setup error. It was close to the findings of Hu Jian et al. [38] that compared the automatic registration of cone beam CT (CBCT) with automatic + manual registration in head and neck tumors, and

the difference was not statistically significant. In the study by Amer et al. [39] the residual errors for head and neck tumors were rather small, which can be explained by the use of a small region of interest for automatic matching due to the limited collimator size of the Beam modulator in the Elekta Synergy system Boswell et al. [36] used HT airborne MVCT to analyze the impact of automatic and manual registration methods on head membrane body treatment error values. During the 1872-step automatic registration process, it was found that 2.5% of the treatment error values exceeded 10 mm. On the other hand, when using manual registration, all treatment error values were below 6 mm, showing that the manual registration method resulted in smaller treatment errors compared to the automatic registration method.

#### **Cervical cancer cases**

In the context of cervical cancer patients, this study found a statistically significant difference between the two registration methods. These findings indicate that relying solely on simple automatic registration of bone and soft tissue is insufficient to meet the requirements for precise treatment in this particular patient group. Additional measures or more advanced registration techniques may be necessary to achieve the desired level of treatment precision for cervical cancer patients. Manual adjustment is necessary based on specific conditions, and is more effective than solo auto registration. The reason may be that, unlike head and neck tumors, abdominal and pelvic tumors are more affected by physiological activity and the filling of the diaphragm, intestine, bladder, and rectum than head and neck tumors, which makes the need for manual registration more apparent. Laursen et al. [40], Cao Qianqian et al. [41], and Wang Xiaoyun et al. [42] used vacuum pads to fix the body position, and conducted CBCT-guided radiotherapy for cervical cancer and endometrial cancer. The MPTV on the x, y, and z axes are 9.6, 8.2, 11.6 mm, 8.1, 11.4, 12.8 mm, 5.4,

7.3 and 5.7 mm, respectively, while the MPTV in the three directions of Xin et al. [43] under the fixation of the thermoplastic mask are respectively 5.2, 11.0, and 5.6 mm. The above studies all show that the displacement is large in the y- and z-axis directions, and the external boundary of thermoplastic body mold fixation is smaller than that of vacuum pad fixation. In this study, the MPTV in the three directions under AR+MR and the thermoplastic mask fixation were 3.351, 4.179, and 5.113 mm, respectively, which were smaller than the above CBCT studies. The results were lower than Singh et al. [38], who used EPID image guidance to obtain PTV boundary values of 0.9 cm, 1.0 cm, and 0.6 cm for X, Y, and Z when alignment marker points were added without body fixation. Wu et al. [39] employed CBCT image-guided equipment, requiring MPTV boundary values of 0.39 cm for X, 0.80 cm for Y, and 0.44 cm for Z. The expansion boundary values of X and Y were greater than those of this investigation. Patni et al. [44] used the CBCT image-guided apparatus for estimating the MPTV values. When compared to the values in this study, the expansion boundary values of X, Y, and Z were greater.

Possible reasons would be that all patients in the current study were fixed with thermoplastic masks, emptied their bladders and rectums, and also drank 600 ml of water 1 hour before treatment. In addition, Laursen et al. [40] believe that for patients with para-aortic irradiation systematic errors can cause compromised target coverage which may lead to more and larger abnormal registration treatment error values. In the current study, the registration site does not include the para-aortic lymph node, which may also be the reason for the small MPTV.

Cervical cancer is sensitive to radiation, and the volume of cervical tumors can be reduced by up to 79% with only 30 Gy [45]; the rapid shrinkage of the tumor changes the position of the cervix, causing the uterus to shift downward and forward significantly, and the



bladder between treatments. Moreover, the fullness of the rectum affects the anterior-posterior position of the target area [45, 46], and studies have shown that the external expansion of the head and feet (y-axis) and the anterior-posterior direction (z-axis) are larger. However, the results of this study showed that manual registration followed by automatic one can decrease position change in the anteroposterior direction to prevent outliers in the automatic registration. Definitely, the strict management of the filling status of the bladder and rectum during the experiment also plays an important role in reducing the MPTV.

### GI cases

In this study, the translational and rotational errors for GI patients reduced after AR+MR, and the decrease was significant except for X and Rx. Equally for the MPTV value of CTV to PTV expansion, the external boundary values of X, Y, and Z were 4.183 mm, 9.534 mm, and 7.36 mm in the AR group and 3.785 mm, 5.074 mm and 4.867 mm in AR+MR group, respectively. The values of the expansion boundaries to the left and right were about the same. The AR+MR group had lesser values in the head-foot and ventrodorsal directions compared to the AR group, measuring 4.4 mm and 2.5 mm, respectively. Sá et al. [43] used 3D surface image guidance to reach MPTV boundary values of 8.9 mm, 10.4 mm, and 9.3 mm for X, Y, and Z, respectively. These values were higher than those in the current investigation for AR and AR+MR. The study by Akimoto et al. conducted an error analysis of image-guided pancreatic cancer patients before each treatment. The MPTV values of PTV in the three directions of X, Y and Z were 8.9, 9.8, and 11 mm, respectively. The main reason for the large value is that the pancreatic position changes greatly due to respiratory movement [47]. This study suggests that manual registration should be done in addition to automatic registration, based on the consistent results found. To better manage setup errors and organ motion, especially in the GI

zone, Four-dimensional CT technology could be a valuable option. It applies respiratory gating technology for CT image acquisition and plan design, and can detect the amplitude and direction of tumor movement during the respiratory cycle [48].

The significant gap observed between the actual treatment position and the HT setup position can be attributed to the positioning method employed in HT. In HT, the positioning is typically performed at the virtual isocenter, which is located 700 mm outside the bore. Consequently, the patient is positioned based on the setup lasers outside the bore, while the actual treatment takes place inside the bore. This discrepancy ignores the potential effects of absolute tomotherapy couch sag, which can further contribute to variations in positioning accuracy. It is important to consider and account for these factors to ensure precise and accurate treatment delivery in HT. As a result, the treatment bed board error value is relatively large during the first treatment. By utilizing a correction system for the bed during the initial treatment, any positioning errors in the Z-direction can be automatically recorded and subsequently adjusted in the following treatments. This systematic approach helps minimize Z-direction positioning errors over the course of the treatment. The correction system ensures that the patient is accurately positioned and aligned, leading to improved treatment precision and reduced errors in the Z-direction [49, 50]. The primary cause of setup errors in the z-axis for all patients, including those with HN, cervical, and GI cancers, could be associated with the process of removing upper body clothing and subsequent plate-laying. These actions may lead to muscle contraction in the back, causing changes in the thickness of the human body in the ventrodorsal direction. This contraction can result in an increased z-axis error during registration with the planning image. The contraction of back muscles and the associated changes in body thickness should be considered as potential factors

contributing to setup errors in the z-axis, and measures should be taken to mitigate their impact on treatment accuracy. Correspondingly, the data showed that the maximum range of RX value for AR of cervical and GI patients was higher than  $2^\circ$  ( $2.79^\circ$  and  $2.15^\circ$ , respectively). A previous study demonstrated that the rotation angle  $>2^\circ$  influences the distribution of the planned dose [51]. Therefore, if the setup error angle was greater than  $2^\circ$ , it was necessary to reset the position. By AR+MR method, the maximum range became lower ( $1.6^\circ$  and  $1.4^\circ$ , respectively). The head pad cushion and the vacuum pad wrapped across the chest, abdomen, and most of the thighs, may have contributed to the greater  $R_x$  value. The lower leg and foot of the patient, not being covered by the vacuum pad, may come into direct contact with the carbon fiber plate of the treatment bed. This situation can lead to patient discomfort and potentially contribute to errors in the setup. The patient's dissatisfaction with this arrangement may have influenced their positioning during treatment, potentially resulting in errors. It is important to address patient concerns and discomfort to ensure their cooperation and accurate positioning during treatment.

## Conclusion

HT has entered the era of precision, which can achieve complete coverage of the tumor target area with a high dose according to planning requirements while forming a steep dose drop area around the tumor to reduce the toxicity for normal tissues around the target area. Therefore, if the fixed position of cancer patients is slightly changed during treatment, it will lead to the failure of cancer treatment and the aggravation of normal tissue toxicity.

This study examined the PTV margins for different disease sites in patients undergoing MVCT-based IGRT treatment for HT. In short, the setup error of patients treated with HT using the AR process will be greater than that with AR+MR. The MVCT image guidance system that comes with tomotherapy can

effectively correct the pre-treatment images of patients, and results showed that manual adjustment based on automatic registration is necessary in HT, especially for cervical and GI cases. Therefore, this mistake must be taken seriously, especially in the ventrodorsal direction. The findings of this study suggest that the utilization of AR for MPTV margins is almost sufficient for patients with HN. However, it was observed that the computed MPTV margins for cervical and GI patients were deviated from the clinical margins. With the utilization of daily image guidance, there is a possibility to reduce the margin in cases, where suitable anatomical sites and landmarks are available. By continuously verifying the patient's position and aligning it with the treatment plan using daily image guidance, the need for larger treatment margins can be minimized. This approach allows for more precise targeting of the tumor while sparing surrounding healthy tissues, potentially leading to improved treatment outcomes and reduced side effects. Conversely, in cases of HN, when daily imaging guidance is not possible, the clinical margins used in this protocol, along with immobilization devices, effectively keep the setup errors within the acceptable range. These margins can serve as a reference for non-IGRT setups, but factors like immobilization and contouring techniques should be taken into account.

This study primarily utilizes MVCT to measure position errors during HT and provides an initial estimation of PTV magnification. However, further research is needed to determine how to combine positioning and organ motion errors to obtain a more accurate estimation of PTV magnification.

## Authors' Contribution

HA. Nedaei regarded the first idea of the work. The pilot study was done by DS. Makrani and HA. Nedaei. N. Banaee and G. Geraily accumulate the images and the related writing conjointly offer assistance with

composing the related works. The strategy usage was carried out by HH. Jassim and DS. Makrani. Results and Examination were carried out by DS. Makrani, AR. Khorrami and N. Banaee. The inquiry about work was edited and administered by HA. Nedaei and G. Geraily. All the authors perused, modified, and affirmed the ultimate adaptation of the manuscript.

### Ethical Approval

This work was approved by the ethical committee of the Faculty of Associated of Medical Science, Tehran University of Medical Science, Tehran, Iran with this code: IR.TUMS.IKHC.REC.1401.098.

### Informed Consent

All the participants signed the informed consent.

### Funding

This research leading to these results received funding from the research chancellor of Tehran University of Medical Sciences (TUMS) Tehran, Iran. (Grant number: 1401-02-10-58431).

### Conflict of Interest

None

### References

1. Billiet C, Vingerhoed W, Van Laere S, Joye I, Mercier C, Dirix P, et al. Precision of image-guided spinal stereotactic ablative radiotherapy and impact of positioning variables. *Phys Imaging Radiat Oncol*. 2022;**22**:73-6. doi: 10.1016/j.phro.2022.04.006. PubMed PMID: 35686020. PubMed PMCID: PMC9172170.
2. Yagihashi T, Inoue T, Shiba S, Yamano A, Yamanaoka M, Sato N, et al. Comparing Efficacy Between Robust and PTV Margin-based Optimizations for Interfractional Anatomical Variations in Prostate Tomotherapy. *In Vivo*. 2024;**38**(1):409-17. doi: 10.21873/invivo.13453. PubMed PMID: 38148099. PubMed PMCID: PMC10756445.
3. Han MC, Hong CS, Chang KH, Kim J, Han SC, Kim DW, et al. TomoMQA: Automated analysis program for MVCT quality assurance of helical tomotherapy. *J Appl Clin Med Phys*. 2020;**21**(6):151-7. doi: 10.1002/acm2.12875. PubMed PMID: 32268003. PubMed PMCID: PMC7324692.
4. Costin IC, Marcu LG. Factors impacting on patient setup analysis and error management during breast cancer radiotherapy. *Crit Rev Oncol Hematol*. 2022;**178**:103-25. doi: 10.1016/j.critrevonc.2022.103798. PubMed PMID: 36031175
5. Dekker J, Rozema T, Böing-Messing F, Garcia M, Washington D, De Kruijff W. Whole-brain radiation therapy without a thermoplastic mask. *Phys Imaging Radiat Oncol*. 2019;**11**:27-9. doi: 10.1016/j.phro.2019.07.004. PubMed PMID: 33458273. PubMed PMCID: PMC7807553.
6. Yoram F, Dharsee N, Mkoka DA, Maunda K, Kisukari JD. Radiation therapists' perceptions of thermoplastic mask use for head and neck cancer patients undergoing radiotherapy at Ocean Road Cancer Institute in Tanzania: A qualitative study. *PLoS One*. 2023;**18**(2):e0282160. doi: 10.1371/journal.pone.0282160. PubMed PMID: 36821555. PubMed PMCID: PMC9949626.
7. Thondykandy BA, Swamidas JV, Agarwal J, Gupta T, Laskar SG, Mahantshetty U, et al. Setup error analysis in helical tomotherapy based image-guided radiation therapy treatments. *J Med Phys*. 2015;**40**(4):233-9. doi: 10.4103/0971-6203.170796. PubMed PMID: 26865760. PubMed PMCID: PMC4728895.
8. Isobe A, Usui K, Hara N, Sasai K. The effects of rotational setup errors in total body irradiation using helical tomotherapy. *J Appl Clin Med Phys*. 2021;**22**(7):93-102. doi: 10.1002/acm2.13271. PubMed PMID: 34028944. PubMed PMCID: PMC8292714.
9. Webster A, Appelt AL, Eminowicz G. Image-Guided Radiotherapy for Pelvic Cancers: A Review of Current Evidence and Clinical Utilisation. *Clin Oncol (R Coll Radiol)*. 2020;**32**(12):805-16. doi: 10.1016/j.clon.2020.09.010. PubMed PMID: 33071029.
10. Kupelian P, Langen K. Helical tomotherapy: image-guided and adaptive radiotherapy. *Front Radiat Ther Oncol*. 2011;**43**:165-180. doi: 10.1159/000322420. PubMed PMID: 21625153.
11. Jassim H, Nedaei HA, Geraily G, Banaee N, Kazemian A. The geometric and dosimetric accuracy of kilovoltage cone beam computed tomography images for adaptive treatment: a systematic review. *BJR Open*. 2023;**5**(1):20220062. doi: 10.1259/bjro.20220062. PubMed PMID: 37389008. PubMed PMCID: PMC10301728.
12. Lowe M, Gosling A, Nicholas O, Underwood T,

- Miles E, Chang YC, et al. Comparing Proton to Photon Radiotherapy Plans: UK Consensus Guidance for Reporting Under Uncertainty for Clinical Trials. *Clin Oncol (R Coll Radiol)*. 2020;**32**(7):459-66. doi: 10.1016/j.clon.2020.03.014. PubMed PMID: 32307206.
13. Grégoire V, Guckenberger M, Haustermans K, Legendijk JJW, Ménard C, Pötter R, et al. Image guidance in radiation therapy for better cure of cancer. *Mol Oncol*. 2020;**14**(7):1470-91. doi: 10.1002/1878-0261.12751. PubMed PMID: 32536001. PubMed PMCID: PMC7332209.
  14. Rørtveit ØL, Hysing LB, Stordal AS, Pilskog S. Reducing systematic errors due to deformation of organs at risk in radiotherapy. *Med Phys*. 2021;**48**(11):6578-87. doi: 10.1002/mp.15262. PubMed PMID: 34606630.
  15. Sasaki F, Yamashita Y, Nakano S, Ishikawa M. Verification of patient-setup accuracy using a surface imaging system with steep measurement angle. *J Appl Clin Med Phys*. 2023;**24**(4):e13872. doi: 10.1002/acm2.13872. PubMed PMID: 36537149. PubMed PMCID: PMC10113693.
  16. Unkelbach J, Bortfeld T, Cardenas CE, Grégoire V, Hager W, Heijmen B, et al. The role of computational methods for automating and improving clinical target volume definition. *Radiother Oncol*. 2020;**153**:15-25. doi: 10.1016/j.radonc.2020.10.002. PubMed PMID: 33039428.
  17. Kensen CM, Janssen TM, Betgen A, Wiersema L, Peters FP, Remeijer P, et al. Effect of intrafraction adaptation on PTV margins for MRI guided online adaptive radiotherapy for rectal cancer. *Radiat Oncol*. 2022;**17**(1):110. doi: 10.1186/s13014-022-02079-2. PubMed PMID: 35729587. PubMed PMCID: PMC9215022.
  18. Jhaveri J, Chowdhary M, Zhang X, Press RH, Switchenko JM, Ferris MJ, et al. Does size matter? Investigating the optimal planning target volume margin for postoperative stereotactic radiosurgery to resected brain metastases. *J Neurosurg*. 2018;**130**(3):797-803. doi: 10.3171/2017.9.JNS171735. PubMed PMID: 29676690. PubMed PMCID: PMC6195865.
  19. Zhao J, Zhang M, Zhai F, Wang H, Li X. Setup errors in radiation therapy for thoracic tumor patients of different body mass index. *J Appl Clin Med Phys*. 2018;**19**(3):27-31. doi: 10.1002/acm2.12270. PubMed PMID: 29493070. PubMed PMCID: PMC5978940.
  20. Zhenghuan L, Manya W, Fantu K, Jie D, Yuan C, Qinghe P, et al. Investigation on cone-beam computed tomography-based liver cancer radiotherapy clinical target volume planning target volume margin and analysis of dosimetric differences. *J Rad Res and App Sci*. 2023;**16**:100537. doi: 10.1016/j.jrras.2023.100537.
  21. Stroom JC, Heijmen BJ. Geometrical uncertainties, radiotherapy planning margins, and the ICRU-62 report. *Radiother Oncol*. 2002;**64**(1):75-83. doi: 10.1016/s0167-8140(02)00140-8. PubMed PMID: 12208578.
  22. Van Herk M. Errors and margins in radiotherapy. *Semin Radiat Oncol*. 2004;**14**(1):52-64. doi: 10.1053/j.semradonc.2003.10.003. PubMed PMID: 14752733.
  23. Liu H, Schaal D, Curry H, Clark R, Magliari A, Kupelian P, et al. Review of cone beam computed tomography based online adaptive radiotherapy: current trend and future direction. *Radiat Oncol*. 2023;**18**(1):144. doi: 10.1186/s13014-023-02340-2. PubMed PMID: 37660057. PubMed PMCID: PMC10475190.
  24. Lavrova E, Garrett MD, Wang YF, Chin C, Elliston C, Savacool M, et al. Adaptive Radiation Therapy: A Review of CT-based Techniques. *Radiol Imaging Cancer*. 2023;**5**(4):e230011. doi: 10.1148/rycan.230011. PubMed PMID: 37449917. PubMed PMCID: PMC10413297.
  25. Galluzzi L, Aryankalayil MJ, Coleman CN, Formenti SC. Emerging evidence for adapting radiotherapy to immunotherapy. *Nat Rev Clin Oncol*. 2023;**20**(8):543-57. doi: 10.1038/s41571-023-00782-x. PubMed PMID: 37280366.
  26. Xia WL, Liang B, Men K, Zhang K, Tian Y, Li MH, et al. Prediction of adaptive strategies based on deformation vector field features for MR-guided adaptive radiotherapy of prostate cancer. *Med Phys*. 2023;**50**(6):3573-83. doi: 10.1002/mp.16192. PubMed PMID: 36583878.
  27. Morgan HE, Sher DJ. Adaptive radiotherapy for head and neck cancer. *Cancers Head Neck*. 2020;**5**:1. doi: 10.1186/s41199-019-0046-z. PubMed PMID: 31938572. PubMed PMCID: PMC6953291.
  28. Glide-Hurst CK, Lee P, Yock AD, Olsen JR, Cao M, Siddiqui F, et al. Adaptive Radiation Therapy (ART) Strategies and Technical Considerations: A State of the ART Review From NRG Oncology. *Int J Radiat Oncol Biol Phys*. 2021;**109**(4):1054-75. doi: 10.1016/j.ijrobp.2020.10.021. PubMed PMID: 33470210. PubMed PMCID: PMC8290862.
  29. Niraula D, Sun W, Jin J, Dinov ID, Cuneo K, Jamaluddin J, et al. A clinical decision support system for AI-assisted decision-making in response-adaptive radiotherapy (ARCIIDS). *Sci Rep*. 2023;**13**(1):5279. doi: 10.1038/s41598-023-

- 32032-6. PubMed PMID: 37002296. PubMed PMCID: PMC10066294.
30. Prabhakar R, Laviraj MA, Hareesh KP, Julka PK, Rath GK. Impact of patient setup error in the treatment of head and neck cancer with intensity modulated radiation therapy. *Phys Med.* 2010;**26**(1):26-33. doi: 10.1016/j.ejmp.2009.05.001. PubMed PMID: 19576833.
  31. Zhou Y, Ai Y, Han C, Zheng X, Yi J, Xie C, Jin X. Impact of setup errors on multi-isocenter volumetric modulated arc therapy for craniospinal irradiation. *J Appl Clin Med Phys.* 2020;**21**(11):115-23. doi: 10.1002/acm2.13044. PubMed PMID: 33070426. PubMed PMCID: PMC7700930.
  32. Siebers JV, Keall PJ, Wu Q, Williamson JF, Schmidt-Ullrich RK. Effect of patient setup errors on simultaneously integrated boost head and neck IMRT treatment plans. *Int J Radiat Oncol Biol Phys.* 2005;**63**(2):422-33. doi: 10.1016/j.ijrobp.2005.02.029. PubMed PMID: 16168835.
  33. Hanania AN, Mainwaring W, Ghebre YT, Hanania NA, Ludwig M. Radiation-Induced Lung Injury: Assessment and Management. *Chest.* 2019;**156**(1):150-62. doi: 10.1016/j.chest.2019.03.033. PubMed PMID: 30998908. PubMed PMCID: PMC8097634.
  34. Kang S, Li J, Ma J, Zhang W, Liao X, Qing H, et al. Evaluation of interfraction setup variations for postmastectomy radiation therapy using EPID-based in vivo dosimetry. *J Appl Clin Med Phys.* 2019;**20**(10):43-52. doi: 10.1002/acm2.12712. PubMed PMID: 31541537. PubMed PMCID: PMC6806484.
  35. Swamidas J, Kirisits C, De Brabandere M, Hellebust TP, Siebert FA, Tanderup K. Image registration, contour propagation and dose accumulation of external beam and brachytherapy in gynecological radiotherapy. *Radiother Oncol.* 2020;**143**:1-11. doi: 10.1016/j.radonc.2019.08.023. PubMed PMID: 31564555.
  36. Boswell S, Tomé W, Jeraj R, Jaradat H, Mackie TR. Automatic registration of megavoltage to kilovoltage CT images in helical tomotherapy: an evaluation of the setup verification process for the special case of a rigid head phantom. *Med Phys.* 2006;**33**(11):4395-404. doi: 10.1118/1.2349698. PubMed PMID: 17153418.
  37. McNair HA, Franks KN, Van Herk M. On Target 2: Updated Guidance for Image-guided Radiotherapy. *Clin Oncol (R Coll Radiol).* 2022;**34**(3):187-8. doi: 10.1016/j.clon.2021.10.002. PubMed PMID: 34728132.
  38. Astreinidou E, Bel A, Raaijmakers CP, Terhaard CH, Lagendijk JJ. Adequate margins for random setup uncertainties in head-and-neck IMRT. *Int J Radiat Oncol Biol Phys.* 2005;**61**(3):938-44. doi: 10.1016/j.ijrobp.2004.11.016. PubMed PMID: 15708278.
  39. Amer A, Marchant T, Sykes J, Czajka J, Moore C. Imaging doses from the Elekta Synergy X-ray cone beam CT system. *Br J Radiol.* 2007;**80**(954):476-82. doi: 10.1259/bjr/80446730. PubMed PMID: 17684077.
  40. Laursen LV, Elstrøm UV, Vestergaard A, Muren LP, Petersen JB, Lindegaard JC, et al. Residual rotational set-up errors after daily cone-beam CT image guided radiotherapy of locally advanced cervical cancer. *Radiother Oncol.* 2012;**105**(2):220-5. doi: 10.1016/j.radonc.2012.08.012. PubMed PMID: 23022176.
  41. Cao Q, Zhu L, Wang J, Qu A, Yao L, Zhou S, et al. Assessments setup errors and target margin by 6D couch for primary cervical cancer. *Zhonghua Yi Xue Za Zhi.* 2015;**95**(9):689-92. PubMed PMID: 25976052.
  42. Xiaoyong W, Hui L, Conghua X, Gong Z, Hui Q, Ji C, et al. The setup errors in postoperative radiotherapy for endometrial and cervical cancer by cone beam CT. *Chinese Journal of Radiological Medicine and Protection.* 2014;**34**(7):523-5. doi: 10.3760/cma.j.issn.0254-5098.2014.07.011.
  43. Xin S. Setup errors in cone-beam computed tomography and their effects on acute radiation toxicity in cervical cancer radiotherapy. *Genet Mol Res.* 2015;**14**(3):10937-43. doi: 10.4238/2015.September.21.4. PubMed PMID: 26400321.
  44. Patni N, Burela N, Pasricha R, Goyal J, Soni TP, Kumar TS, Natarajan T. Assessment of three-dimensional setup errors in image-guided pelvic radiotherapy for uterine and cervical cancer using kilovoltage cone-beam computed tomography and its effect on planning target volume margins. *J Cancer Res Ther.* 2017;**13**(1):131-6. doi: 10.4103/0973-1482.199451. PubMed PMID: 28508846.
  45. Van De Bunt L, Jürgenliemk-Schulz IM, De Kort GA, Roesink JM, Tersteeg RJ, Van Der Heide UA. Motion and deformation of the target volumes during IMRT for cervical cancer: what margins do we need? *Radiother Oncol.* 2008;**88**(2):233-40. doi: 10.1016/j.radonc.2007.12.017. PubMed PMID: 18237798.
  46. Kim H, Beriwal S, Huq MS, Kannan N, Shukla G, Houser C. Evaluation of set-up uncertainties with daily kilovoltage image guidance in external beam radiation therapy for gynaecological cancers. *Clin Oncol (R Coll Radiol).* 2012;**24**(2):e39-45. doi: 10.1016/j.clon.2011.09.007. PubMed PMID:

21943780.

47. Akimoto M, Nakamura M, Nakamura A, Mukumoto N, Kishi T, Goto Y, et al. Inter- and Intrafractional Variation in the 3-Dimensional Positions of Pancreatic Tumors Due to Respiration Under Real-Time Monitoring. *Int J Radiat Oncol Biol Phys.* 2017;**98**(5):1204-11. doi: 10.1016/j.ijrobp.2017.03.042. PubMed PMID: 28721905.
48. Kaučić H, Kosmina D, Schwarz D, Čehobašić A, Leipold V, Pedišić I, et al. An Evaluation of Total Internal Motions of Locally Advanced Pancreatic Cancer during SABR Using Calypso® Extracranial Tracking, and Its Possible Clinical Impact on Motion Management. *Curr Oncol.* 2021;**28**(6):4597-610. doi: 10.3390/curroncol28060389. PubMed PMID: 34898575. PubMed PMCID: PMC8628737.
49. Schubert LK, Westerly DC, Tomé WA, Mehta MP, Soisson ET, Mackie TR, et al. A comprehensive assessment by tumor site of patient setup using daily MVCT imaging from more than 3,800 helical tomotherapy treatments. *Int J Radiat Oncol Biol Phys.* 2009;**73**(4):1260-9. doi: 10.1016/j.ijrobp.2008.11.054. PubMed PMID: 19251098. PubMed PMCID: PMC2749998.
50. Tong Y, Gong G, Chen J, Lu J, Liu T, Cheng P, Yin Y. The heterogeneous CTV-PTV margins should be given for different parts of tumors during tomotherapy. *Oncotarget.* 2017;**8**(51):89086-94. doi: 10.18632/oncotarget.21631. PubMed PMID: 29179501. PubMed PMCID: PMC5687671.
51. Gutfeld O, Kretzler AE, Kashani R, Tatro D, Balter JM. Influence of rotations on dose distributions in spinal stereotactic body radiotherapy (SBRT). *Int J Radiat Oncol Biol Phys.* 2009;**73**(5):1596-601. doi: 10.1016/j.ijrobp.2008.12.025. PubMed PMID: 19306757. PubMed PMCID: PMC2688767.